Festugato, L., Peccin da Silva, A., Diambra, A., Consoli, N. C., & Ibraim, E. (2018). Modelling tensile/compressive strength ratio of fibre reinforced cemented soils. *Geotextiles and Geomembranes*, *46*(2), 155-165. https://doi.org/10.1016/j.geotexmem.2017.11.003

Modelling Tensile/Compressive Strength Ratio of Fibre Reinforced Cemented Soils

Lucas Festugato[1]; Anderson Peccin da Silva[2]; Andrea Diambra[3]; Nilo Cesar Consoli[4] and Erdin Ibraim[5]

ABSTRACT: The present work proposes a theoretical model for predicting the splitting tensile strength (q_t) - unconfined compressive strength (q_u) ratio of artificially cemented fibre reinforced soils. The proposed developments are based on the concept of superposition of failure strength contributions of the soil, cement and fibres phases. The soil matrix obeys the critical state soil mechanics concept, while the strength of the cemented phase can be described using the Drucker-Prager failure criterion and fibres contribution to strength is related to the composite deformation. The proposed developments are challenged to simulate the experimental results for fibre reinforced cemented Botucatu residual soil, for 7 days of cure. While the proposed analytical relation fits well the experimental data for this material, it also provides a theoretical explanation for some features of the experimentally derived strength relationships for artificially fibre reinforced cemented clean sands. A parametric study to analyse the effect of adding different fibre contents and fibre properties is provided. The proposed modelling developments also confirm the existence of a rather constant q_t/q_u ratio with moulding density, cement and fibre contents .

[1] Lecturer, DEng, Dept. of Civil Engineering, Federal University of Rio Grande do Sul, Brazil. E-mail: lucas@ufrgs.br

[2] Research Assistant, MEng, Federal University of Rio Grande do Sul, Brazil. E-mail: anderson.peccin@ufrgs.br

[3] Lecturer, PhD, Queen´s School of Engineering, University of Bristol, UK. E-mail: andrea.diambra@bristol.ac.uk

[4] Professor of Civil Engineering, PhD, Dept. of Civil Engineering, Federal University of Rio Grande do Sul, Brazil. E-mail: consoli@ufrgs.br

[5] Reader, PhD, Queen´s School of Engineering, University of Bristol, UK. E-mail: erdin.ibraim@bristol.ac.uk

Keywords: Geosynthetics, modelling, residual soil, Portland cement, fibres, tensile strength, compressive strength, porosity/cement index.

1 INTRODUCTION

The addition of fibres for improving engineering properties of soils has been widely observed in nature over the years, especially with the presence of plant roots. Early studies showed that the inclusion of plant roots into the soil on slopes significantly increased shear strength (Waldron, 1977; Wu *et al.*, 1979). More recently, the addition of artificial fibres has been used in several engineering applications, such as embankments and subgrade stabilisation beneath footings and pavements. In the last decades, an important engineering material has emerged with the advantages of quality control and easy installation: the geosynthetics (Koerner, 2012). Moreover, the inclusion of randomly distributed short fibres has been reported as an effective and cost attractive technique for increasing the strength of near surface soil layers in field applications (e.g. Consoli *et al*., 2009a; Diambra, 2010; Festugato *et al.*, 2015).

Additionally, Portland cement has been widely employed in the enhancement of clayey or granular soils (e.g. Abdulla and Kiousis, 1997a; Ismail *et al*., 2002). The effect of cementation includes an increase in stiffness and peak strength with increasing cement content and density (e.g. Saxena and Lastrico, 1978; Huang and Airey, 1998), as well as a noticeable gain in tensile strength, cohesion and friction angle (e.g. Lade and Overton, 1989). Concerning field applications, Consoli *et al*. (2009a) revealed the importance of the tensile strength of cemented sands, as the failure mechanism of cemented sand top layers vertically loaded begins with tensile stresses.

The coupling of both techniques (cementation and fibre-reinforcement) gave rise to fibre-reinforced cemented soils and it has also been studied by several researchers. The addition of fibres in cemented soils is of particular interest in those sands that show a brittle failure pattern

(Park, 2009). Maher and Ho (1993) showed that the inclusion of randomly oriented fibres into artificially cemented sands caused a significant increase in both friction angle and cohesion, as well as in compressive and tensile strengths for such specimens. The same behaviour has been reported by other authors in clayey soils and fly ash-soil mixtures (Kaniraj and Havanagi, 2001; Tang *et al.*, 2007).

Potential dosage methodologies for soil-cement blends must consider the influence of distinctive variables, such as porosity and quantity of cement. Consoli *et al.* (2010) found out experimentally that an index named porosity/cement ratio (η/C_{iv}) controls the unconfined compressive strength (q_u) through a power relationship for a given soil treated with Portland cement. This relationship was shown to be also adequate for fibre-reinforced cemented specimens (Consoli *et al*., 2011a; Consoli *et al*., 2013a; Festugato *et al*., 2017) [see Eq. (1)].

$$q_u = X \left[\frac{\eta}{{C_{iv}}^{exp}} \right]^Z \quad (1)$$

where porosity (η) is expressed as percentage of the volume of voids divided by total volume of the specimen while volumetric cement content (C_{iv}) is expressed as percentage of the volume of cement divided by the total volume of the specimen, *X*, *Z* and *exp* are parameters that possibly depend on the soil and binder used. Consoli *et al*. (2011a) showed that the exponent *X* depends on the fibre content whereas Consoli *et al.* (2016) found that Z depends exclusively on the type of soil.

Consoli *et al.* (2011b) demonstrated that such index is also useful in controlling splitting tensile strength (q_t). These studies employed the same soil, fibre and Portland cement used in previous research, and a similar power relationship was obtained [see Eq. (2)].

$$q_t = Y \left[\frac{\eta}{{C_{iv}}^{exp}} \right]^Z \quad (2)$$

where *Y*, *Z* and *exp* are parameters that might depend on the soil and binder used. At that moment, Consoli *et al.* (2011b) detected that the power *Z* and the exponent *exp* were the same for both q_u and q_t, but *X* and *Y* were distinct. In order to check if a q_t/q_u relationship for the studied fibre reinforced Botucatu residual soil – Portland cement blend was a function of porosity, cement content or porosity/cement ratio, Consoli *et al*. (2013a) divided Eq. (2) by Eq. (1), yielding a scalar [see Eq. (3)].

$$\frac{q_t}{q_u} = \frac{2.55x10^6\left[\frac{\eta}{C_{iv}^{0.28}}\right]^{-2.90}}{17.96x10^6\left[\frac{\eta}{C_{iv}^{0.28}}\right]^{-2.90}} = 0.14 \quad (3)$$

Accordingly, the authors found out that there was a straight proportionality between tensile and compressive strengths, being independent of porosity, cement content and porosity/cement ratio, which was valid for the whole studied porosity and cement ranges (see Fig. 1 for fibre reinforced Botucatu residual soil – Portland cement blend).

The q_t/q_u ratio of fibre reinforced artificially cemented soils is an important parameter once its existence allows determining q_t knowing q_u or vice versa, considering the whole porosity and volumetric cement content studied. Besides, Consoli *et al*. (2013b) have shown a theoretical framework proving that the friction angle of fibre reinforced cemented granular soil is unique for a given soil and cement and its value is a function only of q_t/q_u. On the other side, the cohesion of cemented granular soil can be determined on both q_u and q_t/q_u.

Consoli *et al*. (2012) developed similar study with fibre reinforced silty soil treated with lime. Result trends by Consoli *et al*. (2012) were similar to the ones obtained by Consoli *et al*. (2013a), as the q_t/q_u relationship for the fibre reinforced silty soil treated with lime yielded a scalar of 0.15. Up to this moment, several authors have developed constitutive modelling approaches concerning fibre-reinforced sands (Villard and Jouve, 1989; Di Prisco and Nova,

1993; Sivakumar Babu *et al*., 2008; Diambra *et al*., 2007; 2010; 2011; 2013; Ibraim *et al*., 2010),cemented sands (Abdulla and Kiousis, 1997b; Vatsala *et al*., 2001) and concrete fibre mixtures (e.g. Samaan et al., 1998; Teng and Lam, 2004). However, there are no theoretical models able to explain the empirical expression for fibre-reinforced cemented sands exposed above.

Diambra *et al.* (2017) presented a theoretical derivation for the strength of three unreinforced artificially cemented granular soils. The authors showed that the concept of superposition of failure strength contributions of the soil and cement phases is effective in predicting the compressive strength of cemented granular soils. Based on this derivation, the present technical paper proposes an extended theoretical modelling framework to predict the compressive and tensile strengths of fibre reinforced artificially cemented soils by considering the individual properties of its constituents: the soil matrix, the cementing phase and the fibres. It will be shown that the proposed developments provide an accurate estimation of the experimental results and that they corroborate the experimental observation of the existence of a unique q_t/q_u ratio independent of moulding density and cement content. The proposed modelling approach will also offer an insight into the physical meaning of the coefficients governing the simple empirical relationships (1) and (2) for the compressive and tensile strengths of fibre reinforced cemented soil and their ratio q_t/q_u in Eq (3), increasing the confidence for their broader use in the engineering practice. This process will allow the establishment of meaningful connections between the governing coefficients of the empirical relationships and relevant material properties, which can provide significant guidance towards the design of specific soil, cement and fibre mixtures to satisfy required strength criteria.

2 THEORETICAL MODEL

2.1 Testing boundary and stress conditions

Typical boundary stress and strain conditions for the unconfined compression and the splitting tensile tests at failure are reported in Fig. 2. The unconfined compression test is in axisymmetric testing conditions (Fig. 2a) and the failure strength (q_u) is equal to the vertically applied stress (σ_z). The stress and strain conditions of a splitting tensile test, in turn, are slightly more complex. A cylinder is placed horizontally and loaded along its cross-section diameter: plane strain loading conditions (ε_y=0) results on the section shown in Fig. 2b. Stress conditions are invariably not uniform within the loaded specimen but we could concentrate on a small finite element at the centre of the disk cross section. The vertical and horizontal principal stresses on this element (σ_z and σ_x) are equals $3q_t$ and q_t, respectively, as theoretically demonstrated by Jaeger *et al.* (2007) and as shown in Fig. 2b.

Differently from Diambra *et al.* (2017), the stress state for both tests is expressed here in terms of maximum shear and mean stress t,s invariants [$t=(\sigma_z- \sigma_x)/2$; $s=(\sigma_z+ \sigma_x)/2$]. In such coordinates system, the stress ratio at failure k_i can be defined as:

$$k_i = \frac{t_i}{s_i} \qquad \text{with } i=u,t \tag{4}$$

where i distinguishes between unconfined compression (u) and tensile (t) testing conditions. By substitution of the boundary stress conditions of Fig. 2 into the definition of t and s, the stress ratios k_u=1 and k_t=2 for the unconfined compression and splitting tensile tests at failure can be derived, respectively.

2.2 Modelling hypothesis

The fibre reinforced cemented soil is considered a composite material made of three separate constituents: the soil matrix, the cementing phase and the fibres. Four main assumptions are introduced for the following modelling developments:

1) The behaviour of the fibre reinforced cemented soil at the failure point is determined by superposing the strength contributions of the three constituent phases;

2) Strain compatibility between the composite and its three constituent phases, soil, cement and fibres, applies.

3) At the composite failure, the soil matrix is at peak conditions, while the cement phase is at failure conditions and the fibres are stretched according the deformation state of the composite material;

4) Fibres are mono-dimensional elastic elements resisting only to tension. Due to filaments orientation caused by compaction, fibres are considered all horizontal.

By using a volumetric averaging approach (Diambra *et al*. 2011, Diambra *et al*. 2013; Diambra and Ibraim 2015), the stress state of the composite material (t,s) can be derived from the failure stress state of the soil matrix (t_m,s_m), the cementing phase (t_c,s_c) and the fibres (t_f,s_f) with the following relationship:

$$\begin{bmatrix} t \\ s \end{bmatrix} = \mu_m \begin{bmatrix} t_m \\ s_m \end{bmatrix} + \mu_c \begin{bmatrix} t_c \\ s_c \end{bmatrix} + \mu_f \begin{bmatrix} t_f \\ s_f \end{bmatrix} \quad (5)$$

where μ_m, μ_c and μ_f are the volumetric concentrations of soil, cement and fibres in the composite material, respectively. It should be noted that the volumetric cement concentration μ_c is equals C_{iv}/100.

2.3 Failure models for constituent phases

2.3.1 Failure for the soil phase

In soil constitutive modelling, it is customary to link the strength of the material with a state parameter (ψ), which quantifies the difference between the current density state from the corresponding one at critical state (Been and Jefferies 1985). It is possible to express the state parameter in terms of the material porosity (η for current porosity and η_{cs} for the corresponding porosity at the critical state) using the following definition:

$$\psi = \frac{\eta_{cs}}{\eta} \tag{6}$$

where ψ<1 represents a state on the loose side of the critical state line (CSL), while ψ>1 represents a state on the dense side of the CSL. Thus, the soil stress ratio at failure can then be expressed by the following expression:

$$\frac{t_m}{s_m} = M^* = M\left(\frac{\eta_{cs}}{\eta}\right)^a \tag{7}$$

where M^* represents the peak strength, M is the critical state strength and a is a model parameter which links the peak strength to the state parameter, ψ.

2.3.2 Failure and stress paths for the cementing phase

It is considered that the strength of the cement phase is simply described by the Drucker-Prager failure criterion, which can be expressed in terms of the maximum shear and mean stresses as follows:

$$t_c = b_c + M_c s_c \tag{8}$$

where the terms b_c and M_c can be linked to both cohesion c_c and friction angle ϕ_c of the cemented phase as follows:

$$b_c = c_c cos\phi_c \quad (9)$$

and

$$M_c = sin\phi_c \quad (10)$$

According to Diambra et al. (2017), the mathematical manipulations of the following section 2.4 and the Appendix require also the knowledge of the stress paths (K_{cu} and K_{ct} for unconfined compression and splitting tensile tests, respectively) followed by the cementing constituents phase during loading. Experimentally observed stress-strain relationship for cemented soil shows a quasi-elastic behaviour up to the peak strength conditions (Consoli *et al*., 2009a). In fact, the strain levels at failure are generally quite low and elastic conditions have been assumed to determine the stress conditions at failure (Jaeger *et al.* 2007). It is supposed herein that fibre reinforced cemented composite soils, their cemented constituent phase and fibres behave under elastic conditions. The elastic stress-strain relationship for fibre reinforced cemented soils can then be written in the following way:

$$\begin{bmatrix}\varepsilon_x\\ \varepsilon_y\\ \varepsilon_z\end{bmatrix} = \frac{1}{E}\begin{bmatrix}1 & -\nu & -\nu\\ -\nu & 1 & -\nu\\ -\nu & -\nu & 1\end{bmatrix}\begin{bmatrix}\sigma_x\\ \sigma_y\\ \sigma_z\end{bmatrix} \quad (11)$$

where E and ν are respectively the Young's elastic modulus and Poisson's ratio of the fibre reinforced cemented soil. By applying the boundary conditions shown in Fig. 2 for either unconfined compression ($\sigma_z=q_u$, $\sigma_y=0$, $\sigma_x=0$) or splitting tensile ($\sigma_z=3q_t$, $\varepsilon_y=0$, $\sigma_x=-q_t$) tests, it is possible to derive the following strain field for the composite material as function of the material strength (q_u or q_t):

$$\begin{bmatrix}\varepsilon_x\\ \varepsilon_y\\ \varepsilon_z\end{bmatrix} = \frac{q_u}{E}\begin{bmatrix}-\nu\\ -\nu\\ 1\end{bmatrix} \text{ for Unconfined Compression tests} \quad (12)$$

and

200 $$\begin{bmatrix}\varepsilon_x\\ \varepsilon_y\\ \varepsilon_z\end{bmatrix} = \frac{-q_t}{E}\begin{bmatrix}2\nu^2+3\nu+1\\ 0\\ 2\nu^2-\nu-3\end{bmatrix}$$ for Splitting Tensile Tests (13).

201 Assuming strain compatibility between the composite material and its constituents, it is
202 possible to impose the strain fields in Eqs. (12) and (13) in the following elastic stress
203 relationship for the cemented soil material:

204 $$\begin{bmatrix}\sigma_{c_x}\\ \sigma_{c_y}\\ \sigma_{c_z}\end{bmatrix} = \frac{E_c}{(1+\nu_c)(1-2\nu_c)}\begin{bmatrix}1-\nu_c & \nu_c & \nu_c\\ \nu_c & 1-\nu_c & \nu_c\\ \nu_c & \nu_c & 1-\nu_c\end{bmatrix}\begin{bmatrix}\varepsilon_x\\ \varepsilon_y\\ \varepsilon_z\end{bmatrix}$$ (14)

205 where E_c and ν_c are respectively the Young's elastic modulus and Poisson's ratio of the
206 cemented constituent phase. Thus, expressions for σ_{c_x} and σ_{c_z} in both unconfined compression
207 and splitting tensile testing conditions can be derived and substituted in the conventional
208 definition of the maximum shear and mean stress t_c, s_c invariants ($t_c=(\sigma_{c_z}-\sigma_{c_x})/2$; $s_c=(\sigma_{c_z}+$
209 $\sigma_{c_x})/2$), in order to obtain the following slopes of the stress paths (K_{cu} and K_{ct} for unconfined
210 compression and splitting tensile tests respectively) for the cementing constituents phase during
211 loading:

212 $$K_{cu} = \frac{t_c}{s_c} = \frac{\sigma_{c_z}-\sigma_{c_x}}{\sigma_{c_z}+\sigma_{c_x}} = \frac{2\nu_c\nu-1+2\nu_c-\nu}{2\nu_c\nu-1+\nu}$$ (15)

213 and

214 $$K_{ct} = \frac{t_c}{s_c} = \frac{\sigma_{c_z}-\sigma_{c_x}}{\sigma_{c_z}+\sigma_{c_x}} = 2\frac{2\nu_c-1}{2\nu-1}$$ (16).

215 These expressions are function of the Poisson's ratios of the fibre reinforced cemented material
216 (ν) and cementing phase (ν_c). Intersection of these stress paths with the failure conditions for
217 the cementing phase in Eq. (8), allows the estimation of the mean stress contribution of the
218 cementing phase:

219 $s_c = \frac{b_c}{K_{ci} - M_c}$ with i=u,t (17)

220 where the index i discriminates between unconfined compression (u) and splitting tensile (t)
221 testing conditions.

222 ### 2.3.3 Failure conditions and strength contributions of the fibres phase

223 Fibres contribution to strength is related to the composite deformation and the stress mobilised
224 in the fibres (σ_f) can be linked to the strain in the generic direction of fibre orientation (ε) by the
225 following relationship:

226 $\sigma_f = E_f . \varepsilon$ (18)

227 where E_f is the elastic modulus of the fibre. Diambra et al. (2007) and Ibraim et al. (2012)
228 found that, for tamped and vibrated fibre reinforced granular soil samples, fibres assumed a
229 preferred horizontal bedding. Hence, it is assumed here for simplicity that fibres are all
230 horizontally and axi-symmetrically oriented, with respect to the configuration imposed during
231 sample preparation which coincides with that represented in Fig. 2a. It follows that, for
232 unconfined compression tests, all the fibres are oriented within a horizontal x-y plane. Thus,
233 taking advantage of stress-strain relationship for the composite material in Eq. (12), it is
234 possible to derive the following equations for the fibre stress components (σ_{fx} and σ_{fz}) at the
235 composite failure conditions:

236 $\sigma_{fx} = E_f . \varepsilon_x = -\frac{E_f \nu q_u}{E} = -2\frac{E_f \nu t_u}{E}$ (19)

237 and

238 $\sigma_{fz} = 0$ (20)

239 which leads to the following expressions of the stress invariants, t_f and s_f, for the fibre phase:

$$t_f = \frac{\sigma_{f_z} - \sigma_{f_x}}{2} = \frac{E_f \nu t_u}{E} \quad (21)$$

and

$$s_f = \frac{\sigma_{f_z} + \sigma_{f_x}}{2} = -\frac{E_f \nu t_u}{E} \quad (22)$$

The loading conditions of a splitting tensile tests are slightly more complex, because the cylindrical sample is placed on its side after fabrication and the plane of fibre bedding is the vertical x-z plane (Fig. 2b). On this plane, the strain state is not uniform but it can be described by the Mohr's circle in Fig.3. Therefore, the stress components of the fibre phase can be computed by integrating the mobilised stress for all orientation within the x-z plane using the following equations:

$$\sigma_{fx} = \frac{2}{\pi} \int_0^{\theta_l} E_f (\varepsilon_x cos^2\theta + \varepsilon_z sin^2\theta) cos\theta d\theta \quad (23)$$

and

$$\sigma_{fz} = \frac{2}{\pi} \int_0^{\theta_l} E_f (\varepsilon_x cos^2\theta + \varepsilon_z sin^2\theta) sin\theta d\theta \quad (24)$$

where θ_l is the angle of zero strain which, using the relationship in Eq.(13), can be determined as:

$$\theta_l = atan\sqrt{-\frac{\varepsilon_x}{\varepsilon_z}} = atan\sqrt{\frac{2\nu^2+3\nu+1}{-2\nu^2+\nu+3}} \quad (25)$$

Solutions of Eqs. (23) and (24) and the further use of relationship (13) lead to:

$$\sigma_{fx} = \frac{-E_f}{E} t_t \frac{sin\theta_l (4cos^2\theta_l + 6\nu - 1)(\nu+1)}{3\pi} \quad (26)$$

and

$$\sigma_{fz} = \frac{E_f}{E} t_t \frac{\left(4cos^3\theta_l + 6\nu cos\theta_l - 9cos\theta_l - 6\nu + 5\right)}{3\pi} \quad (27)$$

which allow to define the fibre stress invariants (t_f and s_f, respectively) for the splitting tensile tests as follows:

$$t_f = \frac{\sigma_{f_z} - \sigma_{f_x}}{2} = \frac{E_f}{E} t_t \frac{[cos\theta_l\left(4cos^2\theta_l + 6\nu - 9\right) + sin\theta_l\left(4cos^2\theta_l + 6\nu - 1\right) - 6\nu + 5](\nu + 1)}{6\pi} = \frac{E_f}{E} t_t K_{ft} \quad (28)$$

and

$$s_f = \frac{\sigma_{f_z} + \sigma_{f_x}}{2} = \frac{-E_f}{E} t_t \frac{[-cos\theta_l\left(4cos^2\theta_l + 6\nu - 9\right) + sin\theta_l\left(4cos^{2\theta_l} + 6\nu - 1\right) + 6\nu - 5](\nu + 1)}{6\pi} = \frac{-E_f}{E} t_t K_{fs} \quad (29)$$

where the terms K_{ft} and K_{fs} are self-defined.

2.4 Strength relationship for fibre reinforced artificially cemented soil

By substituting the assumed strength criteria for the constituents phases in Eq.(5) as detailed in the Appendix, it is possible to obtain the following expressions for the maximum shear stress t_i for the two analysed tests:

$$t_u = \frac{\mu_c b_c \left(K_{cu} - M^*\right)}{\left(1 - M^* - \mu_f \frac{E_f}{E} \nu (1 + M^*)\right)(K_{cu} - M_c)} \quad (30)$$

and

$$t_t = \frac{2\mu_c b_c \left(K_{ct} - M^*\right)}{\left(2 - M^* - 2\mu_f \frac{E_f}{E} \left(K_{ft} + M^* K_{fs}\right)\right)(K_{ct} - M_c)} \quad (31)$$

Using the stress state described in Fig.2, the following expressions for the unconfined compressive (q_u) and tensile (q_t) strengths can then be obtained, respectively:

$$q_u = 2t_u = \frac{2\mu_c b_c \left(K_{cu} - M\left(\frac{\eta_{cs}}{\eta}\right)^a\right)}{\left(1 - M\left(\frac{\eta_{cs}}{\eta}\right)^a - \mu_f \frac{E_f}{E} \nu \left(1 + M\left(\frac{\eta_{cs}}{\eta}\right)^a\right)\right)(K_{cu} - M_c)} \quad (32)$$

$$q_t = \frac{t_t}{2} = \frac{\mu_c b_c \left(K_{ct} - M\left(\frac{\eta_{cs}}{\eta}\right)^a\right)}{\left(2 - M\left(\frac{\eta_{cs}}{\eta}\right)^a - 2\mu_f \frac{E_f}{E}\left(K_{ft} + M\left(\frac{\eta_{cs}}{\eta}\right)^a K_{fs}\right)\right)(K_{ct} - M_c)} \quad (33)$$

Relationships (32) and (33) provide a direct expression of the compressive and tensile strengths of the fibre reinforced cemented soil in terms of the porosity (η), the cement content (μ_c), and fibre content (μ_f) variables, with μ_c = C_{iv}/100. The proposed relationships require nine model parameters relative to the soil (ϕ, a, η_{cs}), to the cementing phase (bc, Mc, which are linked to the cohesion and friction angle c_c and ϕ_c, and ν_c), to the fibres (E_f), and to the elastic properties of the overall composite material (ν and E) as summarised in Table 1. Since the proposed developments refer to unconfined testing conditions only, it appears reasonable to consider the soil porosity at critical state η_{cs} independent of the mean stress level and thus a material constant.

3 MODEL PREDICTIONS

The predictions of the proposed relationships for unconfined compression and tensile strengths have been assessed by direct comparison with experimental data on the following fibre reinforced cemented soil reported in the literature: Botucatu Residual Soil + early strength Portland cement + polypropylene fibres, cured at 7 days (Consoli *et al*. 2013a).

The physical properties and moulding parameters for the material are reported in Tables 2 and 3, respectively.

3.1.1 Selection of model parameters

As shown in Table 1, the model requires the calibration of nine parameters.:. Due to the limitation of the available experimental data on the individual constituents, it was rather impossible to run a thorough calibration procedure to select the values of certain parameters.

Thus, reasonable choices have been performed when necessary, trying to follow evidence from the literature.

The values of the constants relative to the soil matrices (ϕ, η_{cs} and a) have been selected based on triaxial experimental results and the assumed values are indicated in Table 1. The critical state friction angle ϕ and porosity η_{cs} for Botucatu Residual Soil have been derived from published triaxial tests in Heineck *et al*. (2005) and Heineck (2002). The tests were used to establish a relationship between the peak to critical strength ratio (M^*/M) and the state parameter (ψ) in order to determine the model parameter a governing Eq.(7) as shown in Fig. 3. The model parameter a was found to be 3.5 for the studied soil.

Extensive experimental characterisation of the elastic properties of cemented soils by Felt and Abram (1957) suggests values of the Poisson's ratio for cemented sand and silts between 0.22 and 0.31 with a median value of about 0.26, while typical values of Poisson's ratio for mortar matrix are around 0.2, as suggested by Swamy (1971). These values have been assumed in this research for the Poisson's ratio of the composite material v and the cementing phase v_c, leading to values of the cementing phase stress ratio in Eqs. (15) and (16) of K_{cu}=1.19 and K_{ct}=2.5. In absence of experimental data, a value of 32º for the friction angle of the cement phase has been assumed following indication by Leonards (1965), who investigated the static and dynamic frictional properties of plain smooth mortar. While the accuracy of this value cannot be verified, its influence on the model prediction is rather limited and its variation would just result in the need to assume a slightly different value of the binder strength component b_c to obtain a good fit of experimental data. In fact, this last parameter (b_c) was calibrated by fitting three unconfined compressive and tensile strength results randomly selected for each material. A summary of the assumed value for each material is provided in Table 1.

The elastic modulus of the used polypropylene fibres *E*f was 3000 MPa (Heineck *et al.* 2005, Lirer *et al.* 2011, Consoli *et al.* 2013a). Consoli *et al.* (2009b) have shown that the elastic modulus of cemented soils (E) is strongly dependent on porosity (η) and cement content (C_{iv}), particularly in the form of Eq. (34).

$$E = C\left(\frac{C_{iv}}{\eta^{1/\alpha}}\right) \quad (34)$$

The process of calibration of C can be carried out by fitting the value of strength for 3 to 4 random unconfined compressive tests on the studied fibre reinforced sand. For this material, C was found to be equal to 9000 MPa.

3.1.2 Simulations

Comparison between model simulation and experimental data for the unconfined compression strength (q_u) and splitting tensile strength (q_t) is proposed for fibre reinforced cemented Botucatu residual soil in Fig. 5. The data are presented in the strength versus η/C_{iv}^{exp} ratio plot,where $exp=1/a\approx0.28$ in this case as demonstrated in Diambra et al. (2017), while a direct comparison between model prediction and experimental data is proposed in the q_{model}-q_{exp} graphs. The model predicts reasonably well the magnitude of both unconfined compression strength and splitting tensile tests, with these last ones largely lower. The hyperbolic relationship between strength and η/C_{iv}^{exp} ratio is also well captured by the model for both testing modes. The direct comparison between experimental and predicted compressive and tensile strengths (q_{model}-q_{exp}) shows a quite good correlation.

4 DISCUSSION

4.1.1 Parallelism with empirical formula

The proposed relationships (32) and (33) based on theoretical considerations have a different form compared with the empirically based relationships (1) and (2) proposed by Consoli *et al*. (2010) and Consoli *et al*. (2011a,b). However, for the limited range of variation of M^* between 0.5 and 0.65,, it is possible to simplify Eqs. (32) by introducing the following approximation to their bracketed terms

$$\frac{K_{cu}-M^*}{1-M^*-\mu_f\frac{E_f}{E}\nu(M^*+1)} \cong M^*\left(2.07K_{cu}+9.3\,\frac{E_f}{E}\mu_f\right) \tag{35}$$

Still, Eq. (33) can be simplified through the following approximation:

$$\frac{K_{ct}-M^*}{2-M^*-2\mu_f\frac{E_f}{E}(K_{ft}M^*+K_{fs})} \cong M^*\left(0.93K_{ct}+0.02\frac{E_f}{E}\mu_f\right) \tag{36}$$

where *u* and *t* distinguish between unconfined compression (*u*) and tensile (*t*) testing conditions. The use of relationships (35) and (36) allows to consider a linear dependency between the cemented soil strengths (q_u or q_t) and the peak strength of the soil M^* ($M^*=M(\eta_{cs}/\eta)^a$) in Eqs. (32) and (33). This mathematical approximation was obtained by calculating the values of the left-hand terms in Eqs. (35) and (36) for an expected range of model parameters and determining the coefficients on the right-hand side by averaging the best fit data for each considered combination of parameters. The maximum error of this approximation was found to be slightly less than 15%. A similar approximation was proposed by Diambra et al. (2017) and employed in the context of unreinforced cemented granular soils. Equations (32) and (33) can be can be further manipulated to give:

$$q_u = \frac{2\,M\;b_c\,{\eta_{cs}}^a\left(2.07K_{cu}+9.3\,\frac{E_f}{E}\mu_f\right)}{100\,(K_{cu}-M_c)}\left(\frac{\eta}{C_{iv}^{\frac{1}{a}}}\right)^{-a} \tag{37}$$

$$q_t = \frac{M\ b_c\ \eta_{cs}{}^{a}\left(0.93K_{ct}+0.3\frac{E_f}{E}\mu_f\right)}{100\ (K_{ct}-M_c)}\left(\frac{\eta}{C_{iv}{}^{\frac{1}{a}}}\right)^{-a} \quad (38)$$

As shown in Fig. 6, where the strengths are plotted again versus an adjusted porosity/cement content ratio $\eta/C_{iv}{}^{1/a} \approx \eta/C_{iv}{}^{0.28}$ as proposed by Consoli *et al*. (2007), the transformation introduced by Eq. (31) and (32) has a limited effect on the model predictions. The newly derived Eqs. (37) and (38) are of very similar form to the experimentally derived strength relationships in Eqs. (1) and (2) by Consoli *et al.* (2009b) and Consoli *et al.* (2010). The value of the exponent 1/*a* corroborates also the experimental findings from experimental data by Consoli et al. (2013a) for fibre reinforced Botucatu residual soil in Eq (3) and in Fig. 1.

The parameter *a* of the proposed model corresponds to the power $^{-Z}$ in Eqs. (1) and (2) and it confirms that the same value of the exponent $^{-Z}$ controls the strength in unconfined compression and tension testing conditions. Although this parameter is not exactly the same as the one found from UCS and STS tests by Consoli *et al*. (2013a), the values are close enough to reproduce the experimental data in an effective way. The model also suggests that this parameter is entirely governed by the soil matrix. On the other hand, the parameters *X* and *Y* in Eqs (1) and (2) differ between them in the two testing modes, as also confirmed by the modelling developments, and they can be expressed as:

$$X = \frac{2\ M\ b_c\ \eta_{cs}{}^{a}\left(2.07K_{cu}+9.3\frac{E_f}{E}\mu_f\right)}{100\ (K_{cu}-M_c)} \quad (39)$$

and

$$Y = \frac{M\ b_c\ \eta_{cs}{}^{a}\left(0.93K_{ct}+0.3\frac{E_f}{E}\mu_f\right)}{100\ (K_{ct}-M_c)} \quad (40)$$

for unconfined compression and tension testing conditions, respectively. The two terms are governed by a combination of factors related to both the soil matrix, the fibre reinforcement and the cementing phase.

4.1.2 Effect of fibre content and properties

The effect of fibre content and properties on the strength of fibre reinforced cemented soil can be easily studied by analysing the terms X and Y in Eqs (39) and (40). For a given moulding density and cement content, these terms govern the compressive tensile strength as shown in Eq. (37) and (38). It is possible to investigate the strength increase provided by the fibres by plotting the % increase of these two parameters in relation to the case of no fibres (μ_f=0%) versus the fibre content as shown in Figure 7a. The values of model parameters given in Table 1 have been used in this exercise. Addition of fibres leads to a limited increase in strength, which for unconfined compression can overcome 15% only if large amounts of fibres are used (μ_f=5%). For tensile tests, the increase is much more limited reaching only 0.5% at μ_f=5%. This is related to the much lower proportion of fibre engaged in tension for this loading condition. Using stiffer fibres has also a positive influence on the increase of the compressive strength. as shown in Fig 7b. Full matrix to fibre bonding and absence of shear strain gradients around the fibres (Diambra and Ibraim, 2015) have been assumed in this work. However, fibre aspect ratio, length and fibre to matrix stiffness ratio affect the fibre to matrix stress transfer mechanism. Diambra and Ibraim (2015) have shown that increasing the aspect ratio or the length of the fibres has a beneficial interaction effect and would produce a similar trend of increasing strength as the one associated with an increase of fibre stiffness. However, its accurate quantification would require additional and more complex theoretical developments.

4.1.3 Tensile to compressive strength ratio

Combination of relationship (39) and (40) allows to achieve an explicit relationship between tensile and compressive strength of the cemented soil:

404 $$\frac{q_t}{q_u} = \frac{1}{2}\frac{\left(2.07K_{cu}+9.3\frac{E_f}{E}\mu_f\right)(K_{cu}-M_c)}{\left(0.93K_{ct}+0.3\frac{E_f}{E}\mu_f\right)(K_{ct}-M_c)} \quad (41)$$

405 which is mainly dependent on the strength contribution of the cement phase through the stress
406 path slope K_i and the cement friction ratio M_c. Substitution of the parameters used in this
407 research led to q_t/q_u = 0.156 for the cemented fibre reinforced Botucatu Residual Soil. This
408 value is very similar with the q_t/q_u = 0.14 found by the unconfined compressive tests and
409 splitting tensile tests in Consoli *et al*. (2013a) for this mixture. The theoretical variation of this
410 ratio with the fibre content is provided in Fig. 8. Increasing the fibre content result in a slightly
411 lower value of this ratio which would theoretically decrease to 0.136 for a fibre content μ_f=5%.
412 This decrease is related to the less proportion of fibres engaged in tension for splitting tensile
413 tests. Nevertheless, the influence of fibre content on this ratio appears rather limited. The
414 values plotted in Fig.8 are also all rather close to the experimental ratio found by Consoli *et al*.
415 (2013a),

416 .

417 **5 CONCLUSIONS**

418 This publication proposes a new theoretical derivation for both unconfined compression and
419 splitting tensile strengths based on the concept of superposition of failure strength contribution
420 of the soil matrix, cementing bond and fibre reinforcement phases. The validity of the model
421 has been shown by the comparison of model simulations with fibre-reinforced cemented
422 Botucatu residual soil, which agreed well with the hyperbolic relationship plotted between
423 UCS and STS versus the adjusted porosity/cement index. The model has also confirmed some
424 important material insights:

- The hyperbolic relationships presented in Eqs (1) and (2) of unconfined compression (q_u) and splitting tensile (q_t) strengths versus the porosity/cement index (η/C_{iv}) are characterised by the same exponent power Z which does not depend on the two test loading conditions. This has been theoretically explained by the proposed model which also suggests that this exponent is entirely governed by the soil matrix. Soil matrix properties seem to control this power *Z*.
- The scalars *X* and *Y* in the typical hyperbolic relationships (Eqs (1) and (2)) vary between unconfined compression and splitting tensile conditions. The model suggests that this variation is related to the different stress path between these two types of tests. They are also affected by strength of the sand matrix, cement phase, fibre content and fibre stiffness.
- The model yields to a constant tensile to compression strength ratio (q_t/q_u) which is rather close to what experimentally observed. This ratio is only slightly dependent on the fibre content.

Acknowledgments

The authors gratefully acknowledge the support provided by the UK Royal Academy of Engineering under the Newton Research Collaboration Programme, (Grant reference: NRCP1415/2/2) and by the Brazilian Council for Scientific and Technological Research/Brazilian Ministry of Science and Technology (CNPq/MCT) (Grant reference: 308050/2015-0).

APPENDIX. Derivation of Equations (30) and (31)

The volumetric averaging approach (Diambra *et al*. 2011, Diambra *et al*. 2013; Diambra and Ibraim 2015) in Eq.(5) suggests the following relationship between the stress state of the composite material and its constituents:

$$\begin{bmatrix} t_i \\ s_i \end{bmatrix} = \mu_m \begin{bmatrix} t_m \\ s_m \end{bmatrix} + \mu_c \begin{bmatrix} t_c \\ s_c \end{bmatrix} + \mu_f \begin{bmatrix} t_f \\ s_f \end{bmatrix} \quad \text{(A1)}$$

where the subscript i discriminate between UCS and STS, $i=u$ and $i=t$ respectively. Re-arranging the second line of Eq.(A1), it is possible to write

$$s_m = \frac{s_i - \mu_c s_c - \mu_f s_f}{\mu_m} \quad \text{(A2)}$$

Considering the failure criterion for the soil matrix in Eq. (7) and substituting (A2) in the first line of (A1)

$$t_i = \mu_m M^* \left(\frac{s_i - \mu_c s_c - \mu_f s_f}{\mu_m}\right) + \mu_c t_c + \mu_f t_f \quad \text{(A3)}$$

including the strength criterion for the cement phase (name equations) in (A3) and considering the stress path of the composite in Eq(4)

$$t_i = M^* \frac{t_i}{k_i} - \mu_c M^* \frac{b_c}{K_{ci} - M_c} - \mu_f M^* s_f + \mu_c b_c \left(1 + \frac{M_c}{K_{ci} - M_c}\right) + \mu_f t_f \quad \text{(A4)}$$

This equation can now be simplified to obtain:

$$t_i = M^* \frac{t_i}{k_i} + \mu_c b_c \frac{K_{ci} - M^*}{K_{ci} - M_c} + \mu_f \left(t_f - M^* s_f\right) \quad \text{(A5)}$$

Substituting the formulation for the stress invariants in the fibres (Eqs. (22) and (23) for unconfined compression tests and Eqs (29) and (30) for splitting tensile tests) and the stress paths of the composite materials in Eq(a), and re-arranging, it is possible to derive the following expressions of the maximum shear stress for the two types of test:

$$t_u = \frac{\mu_c b_c \left(K_{cu} - M^*\right)}{\left(1 - M^* - \mu_f \frac{E_f}{E} \nu (1 + M^*)\right)(K_{cu} - M_c)} \quad \text{(A6)}$$

and

467 $$t_t = \frac{2\mu_c b_c\,(K_{ct} - M^*)}{\left(2 - M^* - 2\mu_f \frac{E_f}{E}\left(K_{ft} + M^* K_{fs}\right)\right)(K_{ct} - M_c)} \quad \text{(A7)}$$

468

469

470

471

References

Abdulla, A. A. and Kiousis, P. D. (1997a). “Behavior of cemented sands – I. Testing.” *International Journal for Numerical and Analytical Methods in Geomechanics*, 21(8), 533-547.

Abdulla, A. A. and Kiousis, P. D. (1997b). “Behavior of cemented sands – II. Modelling.” *International Journal for Numerical and Analytical Methods in Geomechanics*, 21(8), 549-568.

Been, K. and Jefferies, M.G. (1985). "A state parameter for sands." *Géotechnique*, 35(2), 99-112.

Consoli, N.C. (2014). “A method proposed for the assessment of failure envelopes of cemented sandy soils”. *Engineering Geology*, 169, 61-68.

Consoli, N.C.; Corte, M.B. and Festugato, L. (2012). “Key parameters for tensile and compressive strength of fiber-reinforced soil-lime mixtures.” *Geosynthetics International*, 19, 409-414.

Consoli, N.C.; Foppa, D.; Festugato, L. and Heineck, K.S. (2007). “Key parameters for strength control of artificially cemented soils”. *Journal of Geotechnical and Geoenvironmental Engineering*, 133(2), 197-205.

Consoli, N.C.; Dalla Rosa, F. and Fonini, A. (2009a). “Plate load tests on cemented soil layers overlying weaker soil”. *Journal of Geotechnical and Geoenvironmental Engineering*, 135(12), 1846-1856.

Consoli, N.C.; Viana da Fonseca, A.; Cruz, R.C. and Heineck, K.S. (2009b). “Fundamental parameters for the stiffness and strength control of artificially cemented sand”. *Journal of Geotechnical and Geoenvironmental Engineering*, 135, 1347-1353.

Consoli, N.C.; Cruz, R.C.; Floss, M.F. and Festugato, L. (2010). “Parameters controlling tensile and compressive strength of artificially cemented sand”. *Journal of Geotechnical and Geoenvironmental Engineering*, 136, 759-763.

Consoli, N. C.; Zortea, F.; Souza, M. and Festugato, L. (2011a). “Studies on the dosage of fiber-reinforced cemented soils.” *Journal of Materials in Civil Engineering*, 23(12), 1624-1632.

Consoli, N.C.; Moraes R.R. and Festugato, L. (2011b). “Split tensile strength of monofilament polypropylene fiber-reinforced cemented sandy soils.” *Geosynthetics International*, 18, 57-62.

505 Consoli, N.C.; Moraes R.R. and Festugato, L. (2013a). “Variables controlling strength of fibre-
506 reinforced cemented soils.” *Proceedings of the ICE - Ground Improvement*, 166, 221-232.
507 Consoli, N.C.; Consoli, B.S. and Festugato, L. (2013b). “A practical methodology for the
508 determination of failure envelopes of fiber-reinforced cemented sands.” *Geotextiles and*
509 *Geomembranes*, 41, 50-54.
510 Consoli, N. C., Samaniego, R. A. Q., Marques, S. F. V., Venson, G. I., Pasche, E. and
511 Velásquez, L. E. G. (2016). “A single model establishing strength of dispersive clay treated
512 with distinct binders.” *Canadian Geotechnical Journal*, 53, 2072-2079.
513 Di Prisco, C. and Nova, R. (1993). “A constitutive model for soil reinforced by continuous
514 threads.” *Geotextiles and Geomembranes*, 12(2), 161-178.
515 Diambra, A. (2010). “Fibre reinforced sands: experiments and constitutive modelling.” PhD
516 Thesis (Doctor of Philosophy) – Faculty of Engineering, Department of Civil Engineering,
517 University of Bristol, UK, 266 p.
518 Diambra, A.; Ibraim, E.; Muir Wood, D. and Russel, A. R. (2010). “Fibre reinforced sands:
519 experiments and modelling.” *Geotextiles and Geomembranes*, 28, p. 238-250.
520 Diambra, A., Ibraim, E., Peccin, A., Consoli, N.C., Festugato, L. (2017). “Theoretical
521 Derivation of Artificially Cemented Granular Soil Strength.” *Journal of Geotechnical and*
522 *Geoenvironmental Engineering*, 143(5): 04017003.
523 Diambra, A., Ibraim, E. Russell, A.R. and Muir Wood, D. (2011). "Modelling the undrained
524 response of fibre reinforced sands." *Soils and Foundations*, 51(4), 625-636.
525 Diambra, A., Ibraim, E. Russell, A.R. and Muir Wood, D. (2013). "Fibre reinforced sands:
526 from experiments to modelling and beyond." *International Journal for Numerical and*
527 *Analytical Methods in Geomechanics*, 37(15), 2427-2455.
528 Diambra, A. and Ibraim, E. (2015). "Fibre-reinforced sand: interaction at the fibre and grain
529 scale." *Géotechnique*, 65(4), 296-308.
530 Diambra, A.; Russel, A. R.; Ibraim, E. and Muir Wood, D. (2007). “Determination of fibre
531 orientation distribution in reinforced sands.” *Géotechnique*, 57(7), 623-628.
532 Dos Santos, A.P.S., Consoli, N.C. and Baudet, B.A. (2010). "The mechanics of fibre-reinforced
533 sand." *Géotechnique*, 60(10), 791-799.
534 Faro, V.P., Consoli, N.C., Schnaid, F., Thomé, A. and Lopes Jr, L.S. (2015). "Field tests on
535 laterally loaded rigid piles in cemented treated soils." *Journal of Geotechnical and*
536 *Geoenvironmental Engineering*, 141(6), 06015003 (d.o.i.: 10.1061/(ASCE)GT.1943-
537 5606.0001296).

538 Felt, E. J., & Abrams, M. S. (1957). “Strength and elastic properties of compacted soil-cement
539 mixtures.” American Society for Testing and Materials Special Technical Publication
540 Portland Cement Association Research and Development Laboratory Bulletin.
541 Festugato, L.; Consoli, N. C.; Fourie, A. (2015). “Cyclic shear behaviour of fibre-reinforced
542 mine tailings.” *Geosynthetics International*, 22, 196-206.
543 Festugato, L.; Menger, E.; Benezra, F.; Kipper, E. A. and Consoli, N.C. (2017). “Fibre-
544 reinforced cemented soils compressive and tensile strength assessment as a function of
545 filament length.” *Geotextiles and Geomembranes*, 45, 77-82.
546 Floss, M.F. (2012). “Strength and stiffness parameters controlling artificially cemented
547 granular soils.” Ph.D. Thesis, Federal University of Rio Grande do Sul, Porto Alegre, Brazil
548 (in Portuguese).
549 Heineck, K.S. (2002). “Study of the hydraulic and mechanical behaviour of geomaterials for
550 impervious horizontal barriers.” PhD Thesis, Federal University of Rio Grande do Sul,
551 Porto Alegre, Brazil (in Portuguese).
552 Heineck, K.S.; Coop, M.R. and Consoli, N.C. (2005). “Effect of microreinforcement of soils
553 from very small to large shear strains.” *Journal of Geotechnical and Geoenvironmental*
554 *Engineering*, 131(8), 1024-1033.
555 Huang, J. T. and Airey, D. W. (1998). “Properties of artificially cemented carbonate sand.”
556 *Journal of Geotechnical and Geoenvironmental Engineering*, 124(6): 492-499.
557 Ibraim, E.; Diambra, A.; Muir Wood, D. and Russel, A. R. (2010). “Static liquefaction of fibre
558 reinforced sand under monotonic loading.” *Geotextiles and Geomembranes*, 28, p. 374-385.
559 Ismail, M. A., Joer, H. A., Sim, W. H., and Randolph, M. F. (2002b). “Effect of cement type on
560 shear behavior of cemented calcareous soil.” Journal of Geotechnical and
561 Geoenvironmental. Engineering, 128(6), 520-529.
562 Jaeger, J.C., Cook, N.G.W. and Zimmerman, R.W. (2007). "Fundamentals of Rock
563 Mechanics." 4th Edition, Oxford - UK, Blackwell Publishing.
564 Kaniraj, S. and Havanagi, V. (2001). "Behavior of Cement-Stabilized Fiber-Reinforced Fly
565 Ash-Soil Mixtures." *Journal of Geotechnical and Geoenvironmental Engineering*, 127(7),
566 574-584.
567 Koerner, R. M. (2012). “Designing with Geosynthetics.” 6th ed. Bloomington, USA: Xlibris
568 Corp., v. 1.
569 Lade, P. V. and Overton, D. D. (1990). “Cementation effects in frictional materials.” *Journal of*
570 *Geotechical Engineering*, 115(10), 1373-1387.

571 Leonards, G.A. (1965). Experimental study of static and dynamic friction between soil and
572 typical construction materials. Technical report AFWL-TR-65-161. Air Force Weapons
573 Laboratory.
574 Lirer, S.; Flora, A. and Consoli, N.C. (2011). "On the strength of fibre-reinforced soils." *Soils*
575 *and Foundations*, 51(4), 601-609.
576 Maher, M.H. and Ho, Y.C. (1993). "Behavior of fiber-reinforced cemented sand under static
577 and cyclic loads." *Geotechnical Testing Journal*, 16 (3), 330–338.
578 Park, S. S. (2009). "Effect of fiber reinforcement and distribution on unconfined compressive
579 strength of fiber-reinforced cemented sand." *Geotextiles and Geomembranes*, 27, 162-166.
580 Samaan, M., Mirmiran, A., & Shahawy, M. (1998). "Model of concrete confined by fiber
581 composites" *Journal of structural engineering*, 124(9), 1025-1031.
582 Saxena, S. K. and Lastrico, R. M. (1978). "Static properties of lightly cemented sand." *Journal*
583 *of Geotechnical Engineering Division*, 104(GT12), 1449-1464.
584 Sivakumar Babu, G. L.; Vasudevan, A. K. and Haldar, S. (2008). "Numerical simulation of
585 fiber-reinforced sand behavior." *Geotextiles and Geomembranes*, 26, 181-188.
586 Swamy, R. N. (1971). "Dynamic Poisson's ratio of Portland cement paste, mortar and
587 concrete." *Cement and Concrete Research*, 1(5), 559-583.
588 Tang, C.; Shi, B.; Gao, W.; Chen, F. and Cai, Y. (2007). "Strength and mechanical behavior of
589 short polypropylene fiber reinforced and cement stabilized clayey soil." *Geotextiles and*
590 *Geomembranes*, 25, 194-202.
591 Teng, J. G., & Lam, L. (2004). "Behavior and modeling of fiber reinforced polymer-confined
592 concrete". J*ournal of structural engineering*, 130(11), 1713-1723.
593 Vatsala, A.; Nova, R. and Srinivasa Murthy, B. R. (2001). "Elastoplastic model for cemented
594 soils." *Journal of Geotechnical and Geoenvironmental Engineering*, 127(8), 679-687.
595 Villard, P. and Jouve, P. (1989). "Behaviour of granular materials reinforced by continuous
596 threads." *Computers and Geotechnics*, 7, 83-98.
597 Waldron, L. J. (1977). "The shear resistance of root-permeated homogeneous and stratified
598 soil." *Soil Science Society of America Journal*, 41, 843-849.
599 Wu, T. H.; Mckinnel, W. P. Iii and Swanston, D. N. (1979). "Strength of tree roots and
600 landslides on Prince of Wales Island, Ala2ska." *Canadian Geotechnical Journal*, 16(1), 19-
601 33.
602

Notation list

a Parameter linking peak strength to state parameter

b_c Binder strength component

C Constant for elastic stiffness of fibre reinforced cemented soil

c_c Cohesion of the cement phase

C_{iv} Volumetric cement content (expressed in percentage)

E Elastic modulus of the fibre-reinforced cemented sand

E_f Elastic modulus of the fibres

K_{ci} Cement stress ratio (K_{cu} for *UCS* tests and K_{ct} for *STS* tests)

K_{fi} Fibre stress ratio (K_{fu} for *UCS* tests and K_{ft} for *STS* tests)

k_i Stress ratio at failure (k_u for *UCS* tests and k_t for *STS* tests)

K_{sf} Coefficient for stress invariant s_f of the fibre phaseK_{tf} Coefficient for stress invariant t_f of the fibre phase

M Critical state strength ratio for the sand

M_c Slope of the failure line for the cement phase in the q_c -p_c plane

M^* Peak strength ratio for the sand

q_t Unconfined compressive strength for the cemented sand

q_u Unconfined compressive strength for the cemented sand

s Mean stress of the cemented sand

s_c Mean stress of the cement phase

s_f Mean stress of the fibres

s_m Mean stress of the sand matrix

STS Splitting tensile tests

t Maximum shear stress of the cement sand

t_i Maximum shear stress for the tests (t_u for UCS tests and t_t for STS tests)

628 t_c Maximum shear stress of the cement phase

629 t_f Maximum shear stress of the fibres

630 t_m Maximum shear stress of the sand matrix

631 UCS Unconfined compression tests

632 X Multiplying parameter in Empirical relationship (1)

633 Y Multiplying parameter in Empirical relationship (2)

634 Z Exponent of empirical relationships (1) and (2)

635 ε Strain for fibre reinforced cemented soil

636 ϕ Friction angle for the sand matrix

637 ϕ_c Friction angle for the cement phase

638 v Poisson's ratio for cemented sand

639 v_c Poisson's ratio for cement phase

640 μ_c Volumetric cement concentration

641 μ_f Volumetric fibre concentration

642 μ_m Volumetric sand matrix concentration

643 σ Stress for fibre reinforced cemented soil

644 σ_c Stress for the cement phase

645 σ_f Fibres average stress

646 ψ State parameter

647 η Porosity

648 η_{cs} Porosity at critical state

649 θ_l Angle of zero strain for splitting tensile test

650

List of tables

List of figures

TABLES

679 Table 1. Parameters of the proposed model and value assumed for fibre reinforced cemented
680 Botucatu residual soil

Symbol	Variable	Values
ϕ	Critical state friction angle	30.5°
η_{cs}	Critical state soil porosity	30%
a	Parameter governing dependence of soil strength on its density	3.5
b_c	Binder strength component	19 MPa (7 days)
ϕ_c	Cement friction angle	32º
v_c	Cement Poisson's ratio	0.2
v	Composite Poisson's ratio	0.26
Ef	Elastic modulus of the fibres	3000 MPa
E	Elastic modulus of the composite material	$C\left(\frac{C_{iv}}{\eta^{1/\alpha}}\right)$ C=9000 MPa

681

682

683 Table 2. Physical properties of the sand samples

Soil Type	**Botucatu Residual Soil**
Specific gravity	2.63
Medium sand (0.2 mm < diameter < 0.6 mm): %	16.2
Fine sand (0.06 mm < diameter < 0.2 mm): %	45.4
Silt (0.002 mm < diameter < 0.06 mm): %	33.4
Clay (Diameter < 0.002 mm)	5.0
Mean particle diameter, D_{50}: mm	0.16
Liquid limit: %	23
Plastic limit: %	13
Plasticity index: %	10
Uniformity coefficient, C_u	50
Preponderant minerals	Quartz
Soil classification (ASTM 2006)	SC

684

685

686 Table 3. Moulding parameters

Soil	**Botucatu residual soil**
Void ratio (e)	0.64, 0.70, 0.78
Cement content (%)	1, 2, 3, 5, 7, 9, 12
Fibre content (%)	0.5
Cement type	PC III
Moisture content (%)	10
η/C_{iv}	from 7 to 64

687

FIGURES

694 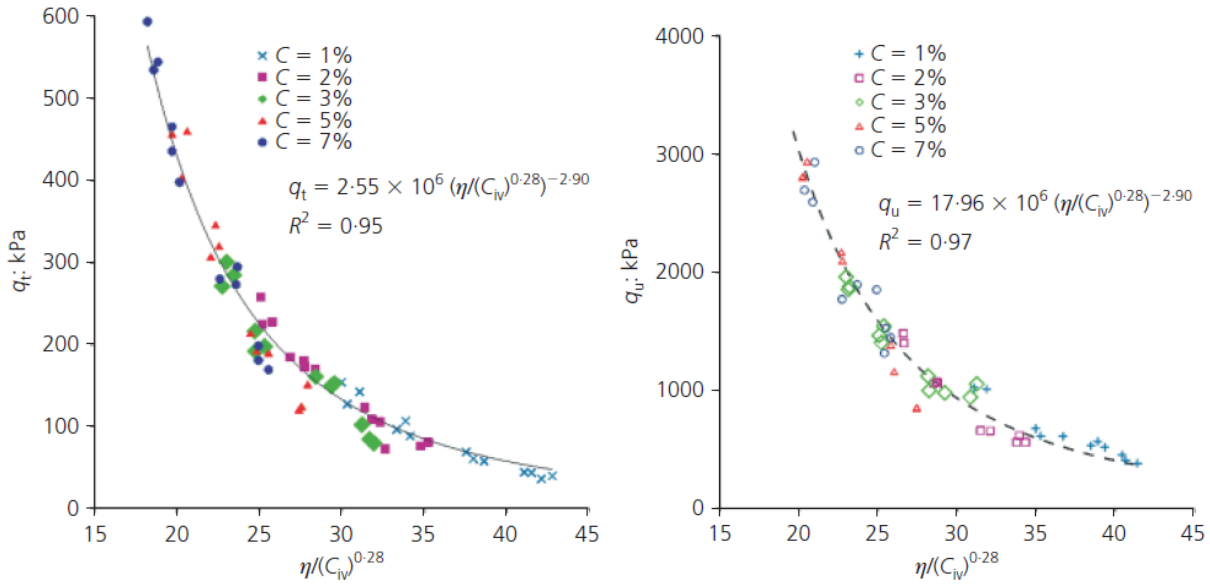

695 (a) (b)

696 Figure 1. Variation of q_t (a) and q_u (b)with porosity/cement ratio for fibre reinforced Botucatu
697 residual soil – Portland cement (adapted from Consoli *et al.* 2013a).

698

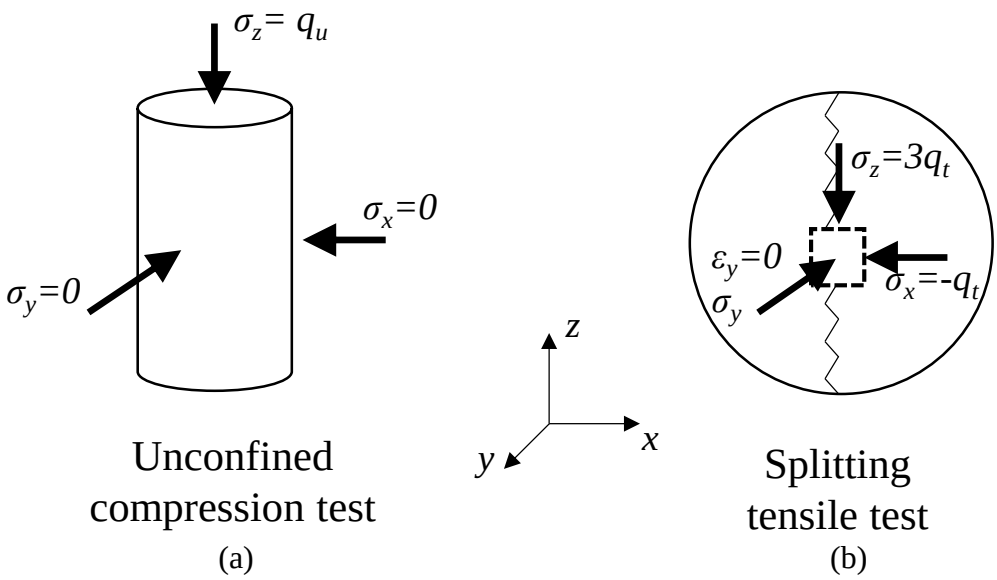

699
700

701

702 Figure 2. Assumed boundary conditions for (a) the unconfined compression test and (b) the
703 tensile splitting test.

704

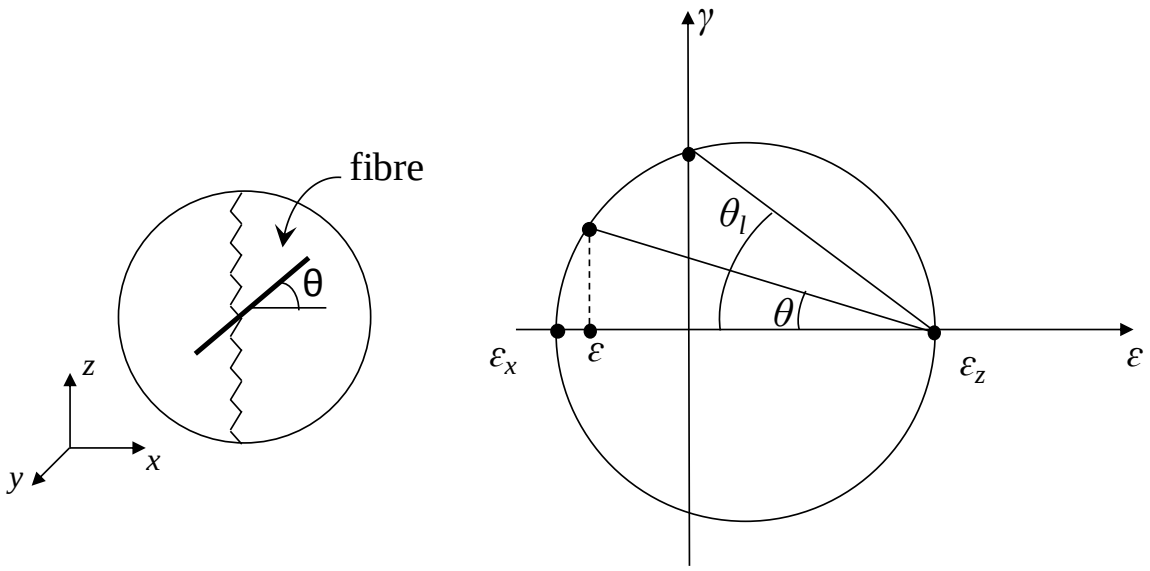

705

706 Figure 3. Representation of strain conditions for the splitting tensile test.

707

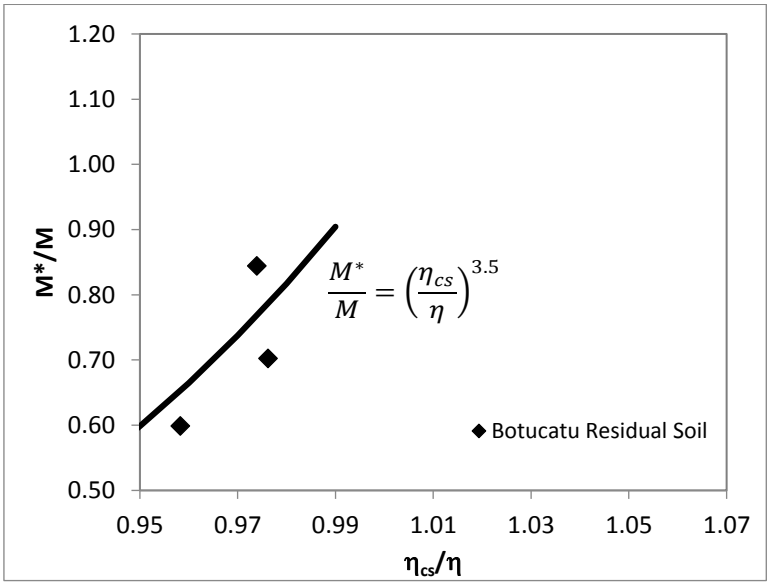

708

709 Figure 4. Calibration of parameter *a* for Botucatu Residual Soil.

710

711

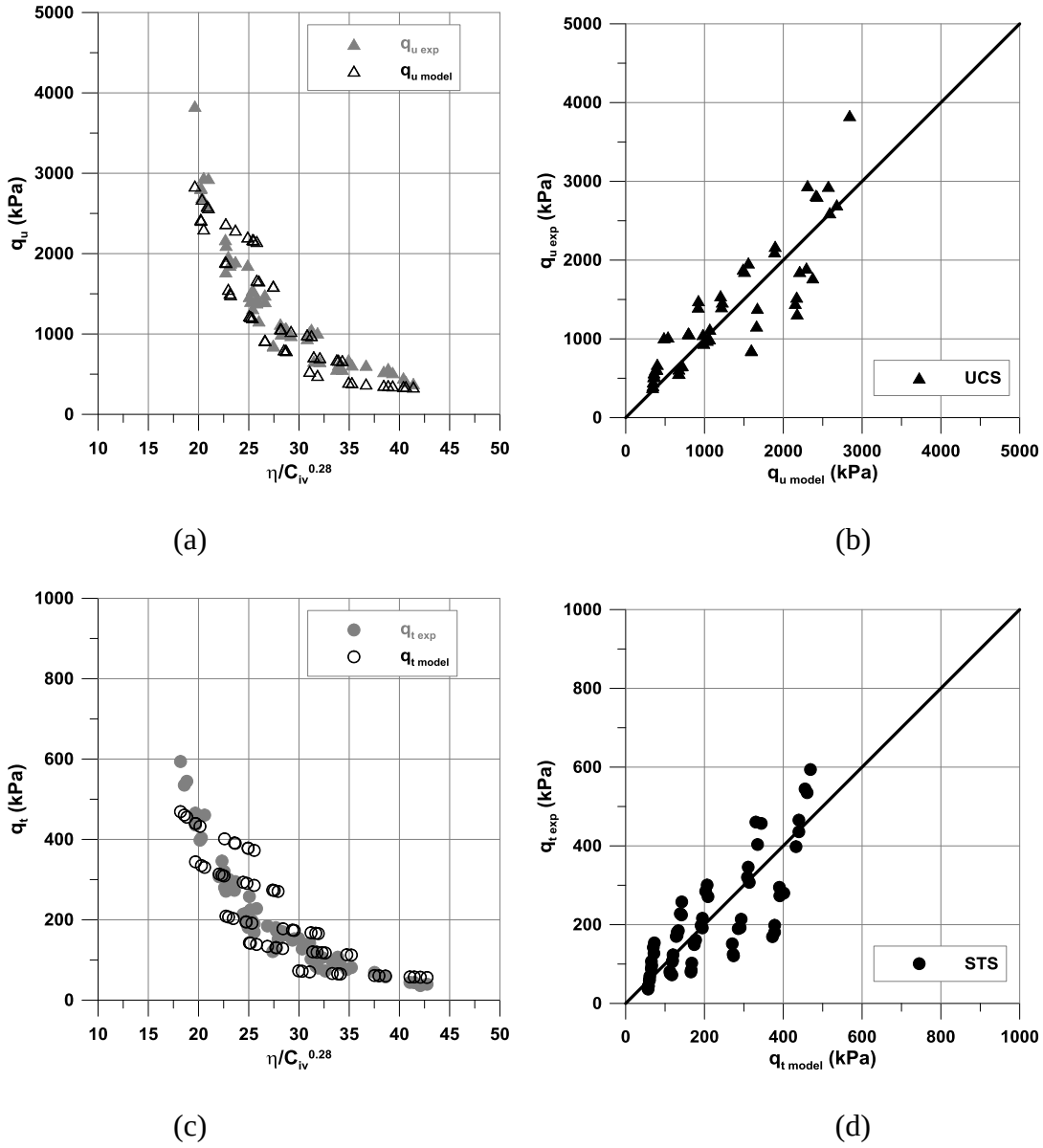

712 Figure 5. Comparison between model prediction and experimental results for UCS and STS of
713 fibre reinforced cemented Botucatu residual soil.

714

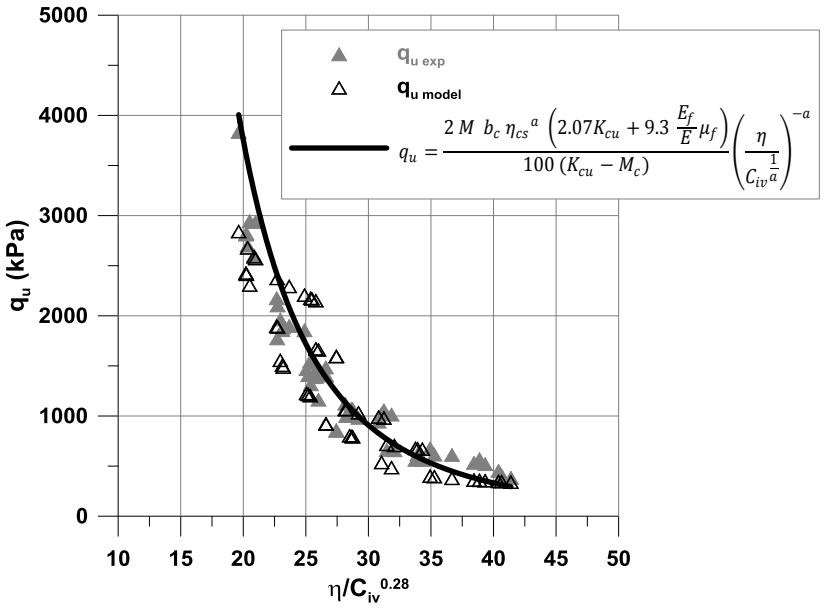

(a)

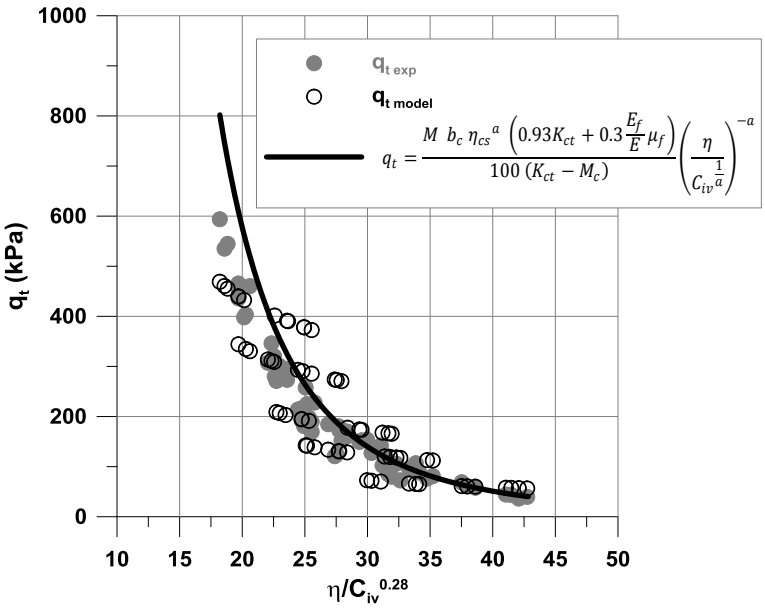

(b)

715 Figure 6. Comparison between experimental data, theoretical prediction and approximated
716 formulas (37) and (38) for fibre reinforced cemented Botucatu residual soil.

717

718

719

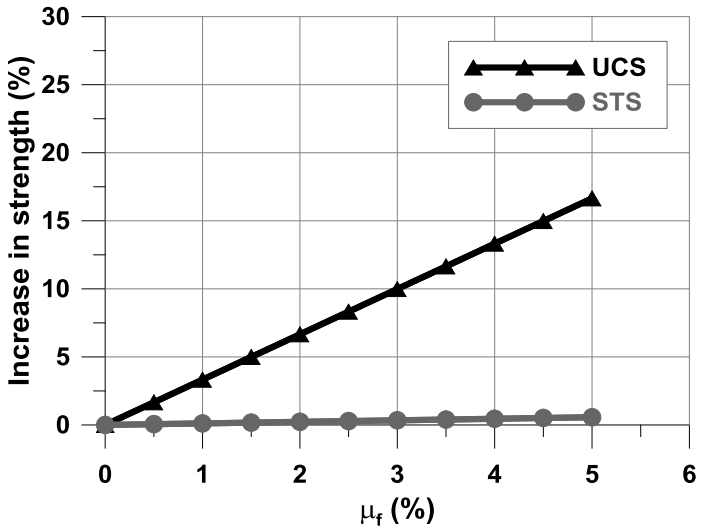

(a)

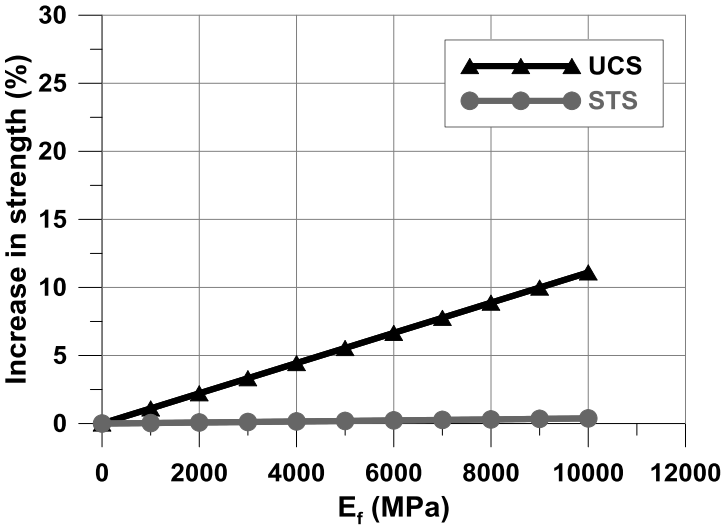

(b)

Figure 7. Theoretical variation of increase in strength with (a) variation of fibre content and (b) variation of fibre elastic modulus

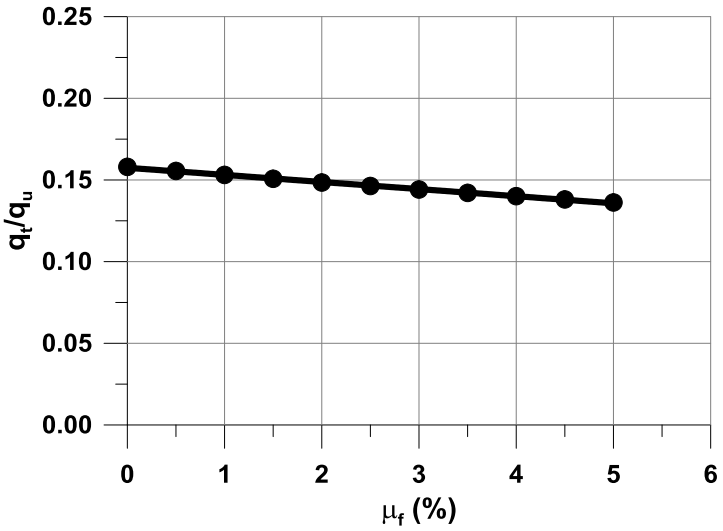

729

730 Figure 8. Theoretical variation of q_t/q_u with variation of fibre content for the values of model
731 parameters in Table 1

732

733